J Mol Model (2001) 7:26–33
DOI 10.1007/s008940100013

ORIGINAL PAPER

Somsak Tonmunphean · Vudhichai Parasuk
Sirirat Kokpol

Automated calculation of docking of artemisinin to heme

Received: 28 September 2000 / Accepted: 1 February 2001 / Published online: 4 April 2001

Abstract We report automated molecular docking of artemisinin to heme. The effects of atomic charges, and ligand and heme structures on the docking results were investigated. Several charge schemes for both artemisinin and heme, artemisinin structures taken from various optimization methods and X-ray data, and five heme models, were employed for this purpose. The docking showed that artemisinin approaches heme by pointing O1 at the endoperoxide linkage toward the iron center, a mechanism that is controlled by steric hindrance. This result differs from that reported by Shukla et al. which suggested that heme binds with artemisinin at the O2 position. The docking results also depended on the structures of both artemisinin and heme. Moreover, the atomic charges of heme have a significant effect on the docking configurations.

Keywords Docking · Antimalarial drug · Endoperoxide · Mechanism of action · Heme

Introduction

Malaria is one of the most widespread and prevalent endemic diseases; it threatens approximately 40 percent of the world's population in more than 90 countries. This disease is estimated to cause approximately 300 to 500 million illnesses and up to 3 million deaths each year [1]. This tremendous prevalence might be partly because of the resistance of malaria parasites to most antimalarial agents, e.g. chloroquine, quinine, and mefloquine [2, 3]. Artemisinin (Fig. 1), a sesquiterpene endoperoxide isolated from a Chinese medicinal herb [4], is, however, a potent antimalarial drug against the resistant strains of *Plasmodium falciparum* [5, 6]. Its unusual structure might be indicative of a different mode of action from those of the other antimalarial drugs, and hence the high potency against the resistant strains. Although the mechanism of its antimalarial activity is still in doubt, there is general agreement on the significance of the endoperoxide group of artemisinin to the antimalarial activity. This is evident from the inactivity of the deoxyartemisinin compound that lacks the endoperoxide moiety [7]. In addition, in-vitro experiments revealed that iron is required for artemisinin to have antimalarial activity [8, 9, 10].

In humans, malarial parasites digest more than 70% of the hemoglobin within the infected red blood cell [11], giving globin and heme as the products. The globin is hydrolyzed to give amino acids, which are used in protein synthesis by the parasite. The toxic heme (Fig. 2) is mostly detoxified by a specific mechanism of heme polymerization into hemozoin. The heme polymerization is a target for some antimalarials, such as chloroquine, that inhibit this process [12]. A recent study reported that artemisinin also inhibits heme polymerization [13]. The chloroquine-resistant strain of *Plasmodium berghei* that lacks hemozoin, possibly because heme polymerization does not occur, is also resistant to artemisinin [14]. This supports the view that inhibition of heme polymerization is the mode of action of artemisinin. It is very possible that artemisinin interacts with heme and hence inhibits the polymerization process.

It has been proposed that heme iron attacks the endoperoxide linkage of artemisinin either at the O1 [15] or

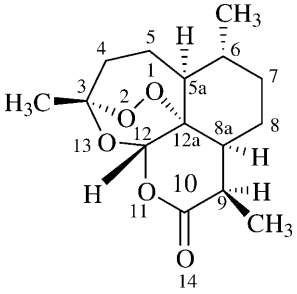

Fig. 1 The structure of artemisinin, with atom numbering

S. Tonmunphean · V. Parasuk (✉) · S. Kokpol
Department of Chemistry, Faculty of Science,
Chulalongkorn University, Patumwan, Bangkok,
10330 Thailand
e-mail: parasuk@atc.atccu.chula.ac.th
Tel.: 662 218 5221, Fax: 662 252 1730

O2 position [16] (Fig. 3). In pathway A, heme iron attacks the compound at the O2 position and produces a free radical at the O1 position. Later it rearranges to form the C4 free radical. In pathway B, heme iron attacks the compound at the O1 position and produces a free radical at the O2 position. After that the C3–C4 bond is cleaved to give a carbon radical at C4. It has been suggested that the C4 free radical in both pathways is an important substance in antimalarial activity [10].

The mechanism of action of any drug is very important in drug development. Generally, the drug compound binds with a specific target, a receptor, to mediate its effects. Therefore, suitable drug–receptor interactions are required for high activity. Understanding the nature of these interactions is very significant and theoretical calculations, in particular the molecular docking method, seem to be a proper tool for gaining such understanding. The docking results obtained will give information on how the chemical structure of the drug should be modified to achieve suitable interactions. Hence, this could bring about the development of new and more effective drugs.

For this reason, Shukla and co-workers [17] studied the docking of artemisinin and deoxyartemisinin with hemin [Fe(II) and Fe(III)] using the Dock module in SYBYL software, a direct docking algorithm. In their study the artemisinin structure was built from the crystallographic X-ray structure of artemether. Although the study did not elaborate on how the structure of artemisinin was obtained from artemether, it is very likely that the geometry optimization was performed at either the molecular mechanics or semi-empirical level, because only these methods are available in SYBYL. For their docking calculations, only three orientations of artemisinin around the hemin molecule were considered. Furthermore, the Gasteiger method, an empirical method implemented in the SYBYL, was used for the atomic charge calculations. Because this empirical method has no parameters for iron, however, the charge of the heme iron was assigned under the assumption that the change in the charge distribution of the heme iron should be equal to that of the heme model where iron was replaced by aluminum. Moreover, the general parameters for metals were used in the docking calculations. The docking scheme they employed might influence the docking result in favor of one of the heme–artemisinin configurations and yield an inaccurate model for the complex. It is quite important to have an accurate model for the heme–artemisinin complex, because this knowledge can be used to design better and more potent antimalarial drugs.

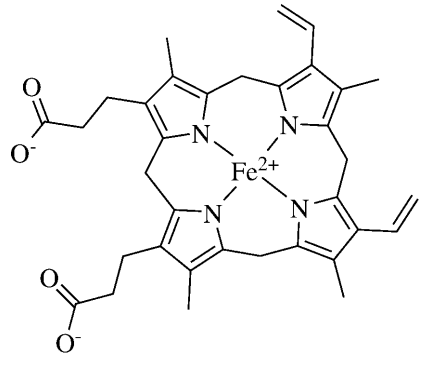

Fig. 2 The structure of heme

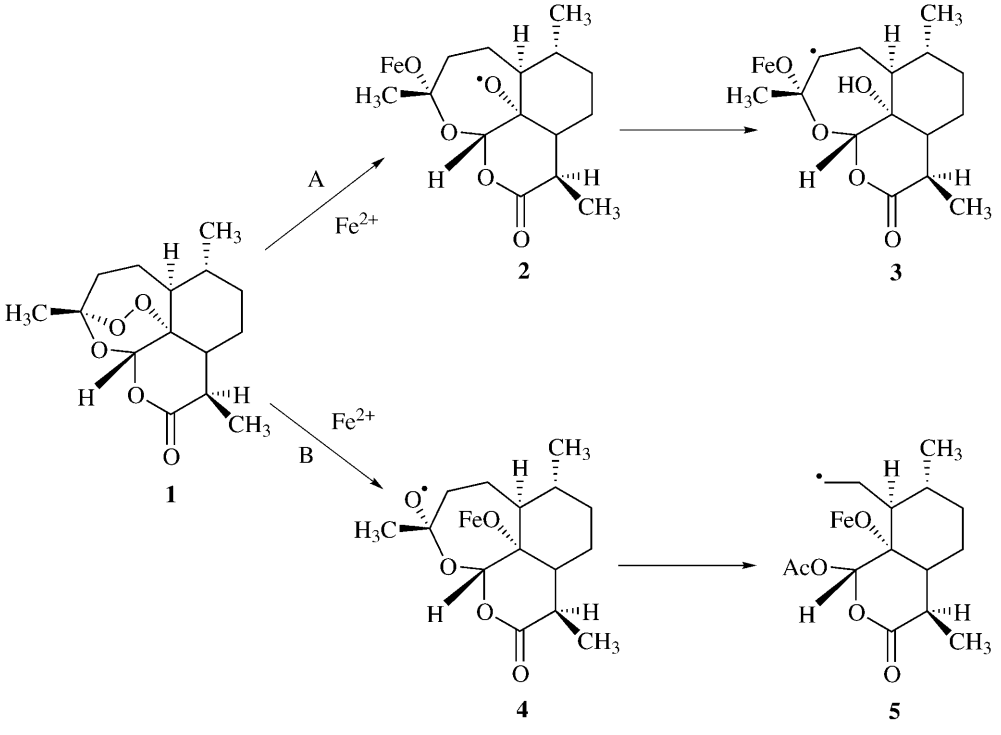

Fig. 3 Proposed mechanism of action of artemisinin

In this study, automated docking calculations were performed to eliminate the bias in selecting preferred configurations (orientations). Thus, all possible configurations between heme and artemisinin were explored. The crystallographic X-ray structure of artemisinin was used for artemisinin instead of that of artemether, which is quite different from the artemisinin structure, especially at the lactone ring. In addition, because few crystallographic X-ray structures of artemisinin derivatives are available, it is worth establishing a suitable geometry optimization scheme to determine structures of artemisinin derivatives for further investigations [18]. For the heme iron, accurate ab initio calculations were performed to obtain its atomic charge (and those of artemisinin) instead of using a crude approximation for the charge of iron, and specific parameters for iron were used in the docking calculations. The effects of different heme structures were also considered. Thus, five heme structures taken from the literature were studied.

The knowledge obtained from this study has been used as a guide for series of docking experiments between heme and artemisinin derivatives and we found a very pronounced relationship between their binding energies and antimalarial activity [18].

Computational details

Docking calculations

AutoDock 2.4 [19], an automated docking program, was used for the docking calculations. The automated docking is performed using a simulated annealing Monte Carlo simulation in combination with a rapid grid-based energy-evaluation method. A grid map of dimensions 25×25×25 $Å^3$ with a 0.5 Å spacing was selected. The combined AMBER/MMFF parameters [20, 21] were chosen for the Lennard–Jones 12,6 potentials and Coulomb potentials to calculate the interaction energy, instead of using the AMBER force field that contains no parameters for iron. These parameters were taken from the authors of the program [22].

In one docking calculation, the simulations were performed for 100 annealing cycles. At the first cycle, the initial annealing temperature (RT) was set to 100 kcal mol^{-1} and then the temperature was reduced at the rate of 0.90 per cycle. During each cycle, the ligand was gradually moved by a random displacement with a maximum translation step of 0.2 Å and a maximum orientation step of 5°. The energy of the new configuration was then calculated. The selection of the new configuration was based on the Metropolis algorithm [23]. The cycle terminates if the ligand makes 30,000 accepted or 30,000 rejected moves. Then the simulation moves to the next cycle.

Because the Monte Carlo simulation is based on random movements, the final docked configuration depends on the starting configuration. To avoid any bias and to generate as many final docked configurations as possible, the starting configuration was assigned randomly for each docking calculation and 100 docking calculations were performed. A cluster analysis was used to categorize all 100 docked configurations into groups. Configurations with root-mean-square-deviation (rmsd) values of less than 1 Å were grouped together. The lowest energy configuration was selected as a representative for each group. Our attention was focused on the group with the highest number of members, referred to as "the most occurring configuration". Thus, it is most probable that this configuration represents the real system.

Ligand and receptor structures

In addition to the crystallographic X-ray structure, the docking of heme and the optimized geometries of artemisinin obtained at AM1, HF/3-21G, and HF/6-31G* levels of theory were investigated (these structures were taken from Ref. [24]). For the receptor molecule, five heme structures, i.e., heme-pdb, heme-model, heme-hemin, heme-deoxy, and heme-oxy, were considered. These structures are all different owing to the source of heme and the oxidation state of iron. The first structure, heme-pdb, was taken from the Protein Data Bank (id 1CTJ) [25]. In this structure, Fe positions itself slightly above the porphyrin plane (Fig. 4a). The second structure, heme-model, which was taken from the AMBER database [26] has the planar geometry (Fig. 4b). The third structure, heme-hemin, was modified from the crystallographic X-ray structure of chlorohemin of the Cambridge Crystallography Data Bank [27]. This structure has a pyramidal shape with Fe on the top (Fig. 4c).

In the process of hemoglobin degradation by the malaria parasite, the proximal ligand may possibly still be attached to the heme iron and, therefore, it is very possible that the histidine remains with the heme structure. As a result, the fourth and the fifth structures, heme-deoxy and heme-oxy, respectively, were obtained from the modifications of deoxy and oxy forms of hemoglobin which contain histidine as the proximal. Both deoxy and oxy forms of hemoglobin were taken from the Protein Data Bank (id 1A3 N and 1HHO, respectively). In the heme-deoxy, the histidine pulls the Fe atom to lie below the protoporphyrin plane and gives it a basin-like structure (Fig. 4d). In the oxy hemoglobin structure, there are six coordinations for heme iron, i.e. with four N atoms in the protoporphyrin ring, with the proximal ligand (histidine), and with O_2. Thus, for docking purposes, the O_2 coordination was deleted while maintaining the coordinates of the rest; this modified structure was taken as the receptor structure. As in heme-deoxy, the protoporphyrin plane has a basin-like structure, because of the attraction to the heme iron by histidine. Interaction with O_2 causes the Fe atom to be drawn up above the plane (Fig. 4e), however, and thus results in a structure which is markedly different from the heme-deoxy.

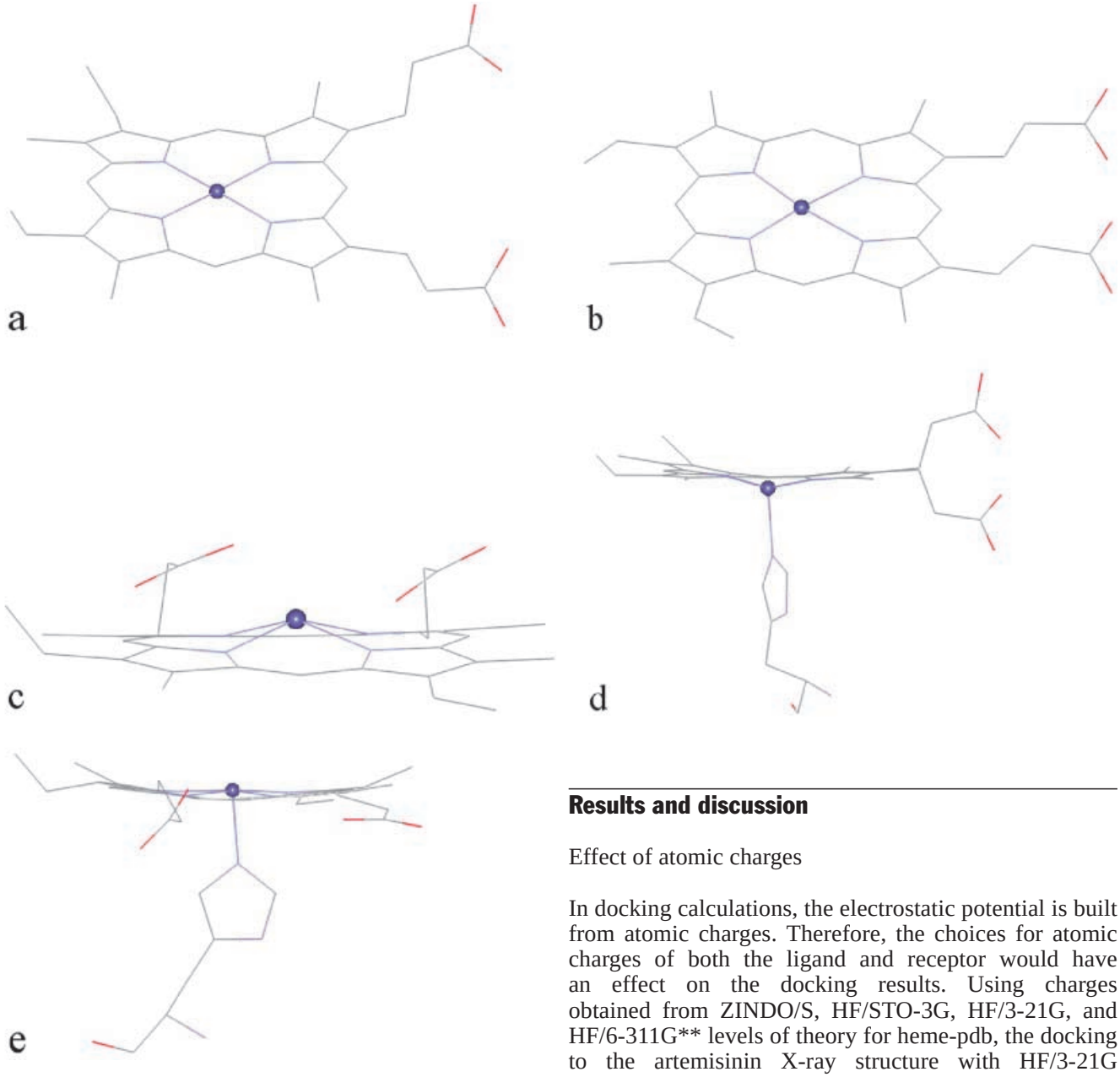

Fig. 4 The structures of the five heme compounds: (**a**) heme-pdb, (**b**) heme-model, (**c**) heme-hemin, (**d**) heme-deoxy, (**e**) heme-oxy

Atomic charge calculations

To investigate the effect of the atomic charge on docked configurations, atomic charges of both artemisinin and heme obtained at various levels of theory were used. For heme, the ZINDO/S, STO-3G, HF/3-21G, and HF/6-311G** atomic charges were calculated. For artemisinin, atomic charge calculations were performed at AM1, PM3, HF/3-21G, HF/D95, HF/6-31G*, and HF/6-311G**. All quantum chemical calculations were carried out using the Gaussian 94 program [28].

Results and discussion

Effect of atomic charges

In docking calculations, the electrostatic potential is built from atomic charges. Therefore, the choices for atomic charges of both the ligand and receptor would have an effect on the docking results. Using charges obtained from ZINDO/S, HF/STO-3G, HF/3-21G, and HF/6-311G** levels of theory for heme-pdb, the docking to the artemisinin X-ray structure with HF/3-21G charges was performed. The results in Table 1 showed that the docking configurations depend on the heme-pdb atomic charges and especially the charge of Fe. With the exception of ZINDO/S charges, all docking calculations agree that the heme iron binds with endoperoxide oxygens, where the O1–Fe distance is the shortest. Among these calculations, docking with HF/6-311G** charges yielded the shortest O1–Fe distance of 2.51 Å. This O1–Fe distance is markedly much shorter than those predicted using HF/STO-3G (2.71 Å) and HF/3-21G (2.70 Å) charges. For the binding energy, the docking with HF/STO-3G charges gave the lowest energy while that with HF/6-311G** charges gave the second lowest. Thus, the employed charge scheme for heme does have a profound effect on the docking result. It is, however, quite difficult to judge which charge scheme leads to the most accurate result, because there is no supporting ex-

Table 1 Results for docking of heme-pdb with different atomic charges and the artemisinin X-ray structure with HF/3-21G charge

Heme-pdb charge	Fe charge	Energy (kcal mol^{-1})	O1–Fe distance (Å)	O2–Fe distance (Å)	O13–Fe distance (Å)	O11–Fe distance (Å)
ZINDO/S	0.127	–30.70	5.50	5.34	3.10[a]	3.64
STO-3G	0.780	–31.57	2.71	3.69	5.45	5.69
HF/3-21G	1.371	–30.44	2.70	3.57	5.41	5.70
HF/6-311G**	1.589	–31.55	2.51	3.09	5.16	5.37

[a] The underlined values are the shortest O–Fe distances

Table 2 Results for docking of heme-pdb with HF/6-311G** charge and the artemisinin X-ray structure with different atomic charges

Artemisininatomic charges	Energy (kcal mol^{-1})	O1–Fe distance (Å)	O2–Fe distance (Å)	O13–Fe distance (Å)	O11–Fe distance (Å)
AM1	–30.70	2.76[a]	3.61	5.41	5.79
PM3	–30.58	2.73	3.59	5.41	5.75
HF/3-21G	–31.55	2.51	3.09	5.16	5.37
HF/D95	–31.71	2.56	3.11	5.19	5.42
HF/6-31G*	–31.40	2.50	3.10	5.16	5.37
HF/6-311G**	–30.58	2.53	3.03	5.10	5.42

[a] The underlined values are the shortest O–Fe distances

Table 3 Atomic charges of four oxygen atoms in artemisinin for all charge schemes

Artemisinin atomic charges	O1 charge	O2 charge	O13 charge	O11 charge
AM1	–0.155	–0.142	–0.289	–0.336
PM3	–0.132	–0.127	–0.252	–0.281
HF/3-21G	–0.374	–0.359	–0.669	–0.710
HF/D95	–0.322	–0.259	–0.489	–0.478
HF/6-31G*	–0.405	–0.368	–0.689	–0.666
HF/6-311G**	–0.333	–0.282	–0.510	–0.461

perimental evidence. Theoretically, HF/6-311G** is the most accurate level of theory employed. It is, therefore, reasonable to choose atomic charges from HF/6-311G** for heme in further docking calculations. To study the effect of atomic charges of artemisinin, the docking calculations using various charge schemes, i.e., AM1, PM3, HF/3-21G, HF/D95, HF/6-31G*, and HF/6-311G** for the artemisinin X-ray structure and HF/6-311G** charges for heme-pdb structure were performed. The docking results are given in Table 2 and the atomic charges of four oxygen atoms in artemisinin for each charge scheme are listed in Table 3. From Table 2, the dockings with ab initio charges (HF/3-21G, HF/D95, HF/6-31G*, and HF/6-311G**) gave similar results, whereas those with semi-empirical charges (AM1 and PM3) gave longer O–Fe distances. Thus, for the sake of saving CPU times, the HF/3-21G charges were chosen for artemisinin.

Effect of artemisinin structure

In our previous study [24], artemisinin was geometry-optimized at various levels of accuracy, ranging from the semi-empirical CNDO and AM1 to ab initio HF/STO-3G, HF/3-21G, and HF/6-31G**. Comparison of these optimized geometries with the crystallographic X-ray structure [29] showed that HF/3-21G gave geometry parameters in good agreement with those of crystallographic X-ray data, especially for the bond length of the endoperoxide linkage, whereas AM1 and HF/6-31G* yielded an O–O bond distance that was too short. This shorter O–O bond length for AM1 and HF/6-31G* is not only found in artemisinin but also in other peroxide systems [30]. The HF/3-21G method is, therefore, recommended for the optimization of artemisinin derivatives. This recommendation is, however, based on geometrical criteria only, which does not necessarily guarantee good docking results.

To validate the use of this optimized artemisinin structure, the docking calculations between heme-pdb with HF/6-311G** atomic charges and the AM1, HF/3-21G, and HF/6-31G* optimized structures of artemisinin were performed. The results were compared with those obtained using the artemisinin crystallographic X-ray structure. For the optimized structures, atomic charges of artemisinin were taken according to the optimization methods, i.e. AM1 charges for the AM1 structure, etc. For the X-ray structure, three docking calculations using AM1, HF/3-21G, and HF/6-31G* charges for artemisinin were performed. The docking results are given in

Table 4 Results for docking of heme-pdb with HF/6-311G** charge and artemisinin optimized structures at various levels of theory

Artemisinin structure	Artemisinin atomic charges	Energy (kcal mol^{-1})	O1–Fe distance (Å)	O2–Fe distance (Å)	O13–Fe distance (Å)	O11–Fe distance (Å)
X-Ray	AM1	–30.70	2.76[a]	3.61	5.41	5.79
	HF/3-21G	–31.55	2.51	3.09	5.16	5.37
	HF/6-31G*	–31.40	2.50	3.10	5.16	5.37
AM1	AM1	–30.60	2.56	3.06	5.16	5.55
HF/3-21G	HF/3-21G	–31.40	2.49	3.12	5.14	5.40
HF/6-31G*	HF/6-31G*	–31.38	2.58	3.13	5.14	5.49

[a] The underlined values are the shortest O–Fe distances

Table 5 Results for docking of different heme structures and artemisinin HF/3-21G optimized structure

Heme	Energy (kcal mol^{-1})	Frequency (%)	O1–Fe distance (Å)	O2–Fe distance (Å)	O13–Fe distance (Å)	O11–Fe distance (Å)
heme-pdb	–31.40	25	2.49 [a]	3.12	5.14	5.40
heme-model	–29.92	22	2.75	3.66	5.38	5.79
heme-hemin	–33.13	24	2.00	2.65	4.67	4.90
heme-deoxy	–31.03	39	5.95	5.53	3.26	4.03
	–30.18	13	3.19	4.18	5.85	6.19
heme-oxy	–32.32	51	2.52	3.32	5.12	5.57

[a] The underlined values are the shortest O–Fe distances

Table 4. Comparison of the configurations which occur most often reveals good agreement between the docking using the X-ray structure and HF/3-21G structure for artemisinin. The largest deviation is 0.03 Å (O11–Fe distance). Comparing the AM1 and the X-ray structures, the optimized structure yielded an O1–Fe distance that was short by 0.2 Å, with the largest deviation 0.55 Å (O2–Fe distance). Although much better for docking than the AM1 structure, when comparing the HF/6-31G* and X-ray structures, the optimized structure gave an O1–Fe distance that was too long by 0.08 Å, with the largest deviation of 0.12 Å (O11–Fe distance). The discrepancy between the docking results obtained from the AM1 and the HF/6-31G* structures and the X-ray structure is clearly rooted in the deficiency of the methods, which yielded O–O distances that were too short. Thus, the method which gives a good structure (compared with the X-ray structure) will also give good docking results. HF/3-21G is, therefore, the recommended method for geometry optimization of artemisinin derivatives in further study although it has a lower level of accuracy than HF/6-31G*. It can be argued that for artemisinin derivatives it is possible that the good agreement between the HF/3-21G and the X-ray structures no longer exists, so it would be wiser to employ the more accurate method, HF/6-31G*. From previous calculations on artemisinin, however, and the current docking results the difference between the structures obtained from the two methods is not pronounced. Thus, the HF/3-21G method is still preferred, because of its faster computation time.

Effect of heme structure

To investigate the effect of the heme structure, five heme structures were selected as described in the section on computational details. The atomic charges were assigned as HF/6-311G** charges for all five heme molecules. For artemisinin compounds, the HF/3-21G optimized structure and atomic charges were used. The results are shown in Table 5 and Fig. 5.

The heme structure chosen does have an effect on the docking results. Although we could not observe agreement on O–Fe distances, all docking calculations with different heme structures (except heme-deoxy) suggested that artemisinin prefers to dock at endoperoxide oxygens (O1 and O2). Using heme-pdb for the heme structure, the docking results showed that artemisinin pointed its endoperoxide moiety toward the heme iron for the most occurring configuration. The O1–Fe and O2–Fe distances of were measured and found to be 2.49 Å and 3.12 Å, respectively (Fig. 5a); the binding energy obtained was –31.40 kcal mol^{-1}. Owing to the planar structure of the heme-model, the repulsion between artemisinin and the protoporphyrin ring of heme prevents artemisinin from approaching the heme iron as closely as for heme-pdb. Thus, the O1–Fe and O2–Fe distances of 2.75 Å and 3.66 Å (Fig. 5b) were obtained, with a binding energy of –29.92 kcal mol^{-1}, the weakest among the heme structures investigated. Unlike the first two models, the distances between the endoperoxide oxygens and Fe for heme-hemin are very short, 2.00 Å and 2.65 Å for O1–Fe and O2–Fe (Fig. 5c), with a binding energy of –33.13 kcal mol^{-1} (the lowest). This is probably because of the pyramidal-like structure of heme-hemin which facilitates the approach of Fe to the endoperoxide moiety.

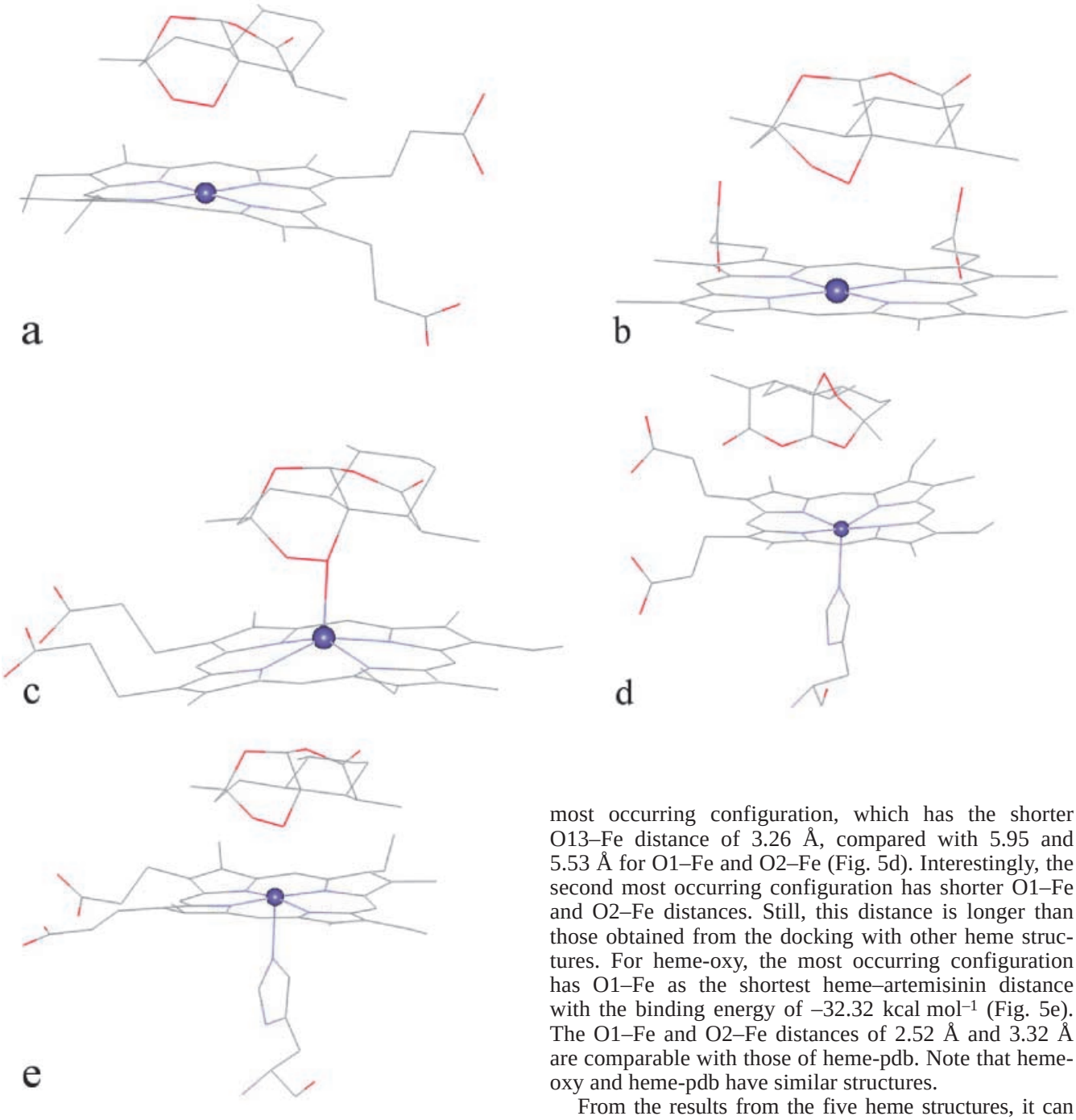

Fig. 5 Docking configuration between artemisinin and (**a**) heme-pdb, (**b**) heme-model, (**c**) heme-hemin, (**d**) heme-deoxy, (**e**) heme-oxy

The O1–Fe distance of 2.00 Å is comparable with the experimental bond length between the heme iron and oxygen atom in oxyhemoglobin A (1.86 Å), taken from the Protein Data Bank (id 1HHO).

For the heme-deoxy, because of its basin-like structure (see Fig. 4d), the binding with the endoperoxide moiety of artemisinin is less favorable and a stronger O13–Fe attraction is resulted (binding energy –31.03 kcal mol^{-1}). This could be observed from the most occurring configuration, which has the shorter O13–Fe distance of 3.26 Å, compared with 5.95 and 5.53 Å for O1–Fe and O2–Fe (Fig. 5d). Interestingly, the second most occurring configuration has shorter O1–Fe and O2–Fe distances. Still, this distance is longer than those obtained from the docking with other heme structures. For heme-oxy, the most occurring configuration has O1–Fe as the shortest heme–artemisinin distance with the binding energy of –32.32 kcal mol^{-1} (Fig. 5e). The O1–Fe and O2–Fe distances of 2.52 Å and 3.32 Å are comparable with those of heme-pdb. Note that heme-oxy and heme-pdb have similar structures.

From the results from the five heme structures, it can be concluded that the structure of the heme molecule has a significant effect on the docking configurations. The steric hindrance at the Fe position plays an important role in the binding. The proximal ligand that increases the steric hindrance at the Fe position would significantly affect the docking results, as in heme-deoxy. If, however, the proximal ligand does not increase the steric hindrance, results similar to those without the proximal ligand, i.e. for heme-oxy and heme-pdb, would be obtained. Therefore, the heme structures which facilitate binding between Fe and endoperoxide oxygens, such as heme-pdb, heme-hemin, and heme-oxy, are recommended for further investigation of the heme–artemisinin system.

All docking calculations similarly reported O1–Fe as the shortest heme–artemisinin distance and O2–Fe as the second shortest. It could then be concluded that iron in heme interacts with O1 more preferably than O2, a preference which might arise from the more negative charge at O1 and the steric hindrance at O2. This observation is in agreement with the proposal of Posner et al. [16] (pathway B). From their docking results, however, Shukla et al. [17] reported O2–Fe as the shortest heme–artemisinin distance. This disagreement is possibly the result of using poor atomic charges, ab initio rather than empirical models, and a poor geometry for artemisinin.

Conclusions

The docking results for five heme structures all agreed that the heme iron approaches the endoperoxide moiety at the O1 position in preference to the O2 position. The docking configuration depends on the structures and atomic charges of both artemisinin and heme. The HF/3-21G level of theory is suitable for the geometry optimization of artemisinin and its derivatives. The docking configurations were significantly affected by the atomic charges of heme and to a much lesser extent by the atomic charges of artemisinin. The high quality atomic charges, 6-311G**, are recommended for the electrostatic potential of heme. Heme structures with no or little steric hindrance at the Fe position facilitate binding of heme and endoperoxide oxygens as in heme-pdb, heme-hemin, and heme-oxy, and they are recommended for use in docking calculations. Comparison of docking results for heme-deoxy and heme-oxy, the heme-oxy structure, whose structure is very close to the receptor structure in the bound state, gave docking results that are in agreement with those of other heme structures.

Acknowledgements The authors would like to thank the Computer Center of the University of Vienna, Austria, for providing computing resources at their workstation clusters and the Austrian-Thai Center (ATC) for Computer-Assisted Chemical Education and Research, Department of Chemistry, Faculty of Science, Chulalongkorn University, Thailand, for computer resources and other facilities. Tonmunphean S. would like to thank Prof. Dr. Peter Wolschann, Institute of Theoretical Chemistry and Molecular Biology, University of Vienna, Austria for helpful discussion and comments.

References

1. World Health Organization. *The World Health Report 1999*.
2. Moore, D. V.; Lanier, J. E. *Am. J. Trop. Med. Hyg.* **1961**, *10*, 5.
3. Mockenhaupt, F. P. *Parasitol. Today* **1995**, *11*, 248.
4. Qinghaosu Antimalaria Coordinating Research Group *Chin. Med. J.* **1979**, *92*, 811.
5. Klayman, D. L. *Science* **1985**, *228*, 1049.
6. Luo, X. D.; Shen, C.-C. *Med. Res. Rev.* **1987**, *7*, 29.
7. China Cooperative Research Group on Qinghaosu and Its Derivatives as Antimalarials *J. Trad. Chin. Med.* **1982**, *2*, 3.
8. Meshnick, S. R.; Thomas, A.; Ranz, A.; Xu, C.-M.; Pan, H.-Z. *Mol. Biochem. Parasitol.* **1991**, *49*, 181.
9. Meshnick, S. R.; Yang, Y.-Z.; Lima, V.; Kuypers, F.; Kamchonwongpaisan, S.; Yuthavong, Y. *Antimicrob. Agents Chemother.* **1993**, *37*, 1108.
10. Posner, G. H.; Oh, C. H.; Wang, D.; Gerena, L.; Milhous, W. K.; Meshnick, S. R.; Asawamahasakda, W. *J. Med. Chem.* **1994**, *37*, 1256.
11. Francis, S. E.; Sullivan, D. J.; Goldberg, D. E. *Annu. Rev. Microbiol.* **1997**, *51*, 97.
12. Slater, A. F. *Pharmacol. Ther.* **1993**, *57*, 203.
13. Pandey, A. V.; Tekwani, B. L.; Singh, R. L.; Chauhan, V. S. *J. Biol. Chem.* **1999**, *274*, 19383.
14. Peters, W.; Li, Z. L.; Robinson, B. L.; Warhurst, D. C. *Ann. Trop. Med. Parasitol.* **1986**, *80*, 483.
15. Jefford, C. W.; Vicente, M. G. H.; Jacquier, Y.; Favarger, F.; Mareda, J.; Millasson Schmidt, P.; Brunner, G.; Burger, U. *Helv. Chim. Acta* **1996**, *79*, 1475.
16. Posner, G. H.; Cummings, J. N.; Ploypradith, P.; Oh. C. H. *J. Am. Chem. Soc.* **1995**, *117*, 5885.
17. Shukla, K. L.; Gund, T. M.; Meshnick, S. R. *J. Mol. Graph.* **1995**, *13*, 215.
18. Tonmunphean, S.; Parasuk, V.; Kokpol S. *Quant. Struct–Act. Rel.* **2000**, *19*, 475.
19. Morris, G. M.; Goodsell, D. S.; Huey, R.; Olson, A. J., AutoDock version 2.4, The Scripps Research Institute, Department of Molecular Biology, MB-5, La Jolla, California, U.S.A.
20. Weiner, S. J.; Kollman, P. A.; Nguyen, D. T.; Case, D. A. *J. Comput. Chem.* **1986**, *7*, 230.
21. Halgren, T. A. *J. Am. Chem. Soc.* **1992**, *114*, 7827.
22. http://www.scripps.edu/pub/olson-web/doc/autoflex/parameters.html
23. Morris, G. M.; Goodsell, D. S.; Huey, R.; Olson, A. J. *J. Comput-Aided Mol. Des.* **1996**, *10*, 293.
24. Tonmunphean, S.; Kokpol, S.; Parasuk, V.; Wolschann, P.; Winger, R. H.; Liedl, K. R.; Rode, B. M. *J. Comput-Aided Mol. Des.* **1998**, *12*, 397.
25. http://www.rcsb.org/pdb/
26. Case, D. A.; Pearlman, D. A.; Caldwell, J. W.; Cheatham, T. E. III; Ross, W. S.; Simmerling, C. L.; Darden, T. A.; Merz, K. M.; Stanton, R. V.; Cheng, A. L.; Vincent, J. J.; Crowley, M.; Ferguson, D. M.; Radmer, R. J.; Seibel, G. L.; Singh, U. C.; Weiner, P. K.; Kollman, P. A. (1997), AMBER 5, University of California, San Francisco.
27. http://www.ccdc.cam.ac.uk/
28. Gaussian 94, Revision B.3, M. J. Frisch, G. W. Trucks, H. B. Schlegel, P. M. W. Gill, B. G. Johnson, M. A. Robb, J. R. Cheeseman, T. Keith, G. A. Petersson, J. A. Montgomery, K. Raghavachari, M. A. Al-Laham, V. G. Zakrzewski, J. V. Ortiz, J. B. Foresman, C. Y. Peng, P. Y. Ayala, W. Chen, M. W. Wong, J. L. Andres, E. S. Replogle, R. Gomperts, R. L. Martin, D. J. Fox, J. S. Binkley, D. J. Defrees, J. Baker, J. P. Stewart, M. Head-Gordon, C. Gonzalez, and J. A. Pople, Gaussian, Inc., Pittsburgh PA, 1995.
29. Leban, I.; Golic, L. *Acta. Pharm. Jugosl.* **1988**, *38*, 71.
30. Bernardinelli, G.; Jefford, C. W.; Maric, D.; Thomson, C.; Weber, J. *Int. J. Quant. Chem. Bio. Sym.* **1994**, *21*, 117.